WATER RESOURCES RESEARCH, VOL. 35, NO. 6, PAGES 1839–1851, JUNE 1999

Ground-based investigation of soil moisture variability within remote sensing footprints during the Southern Great Plains 1997 (SGP97) Hydrology Experiment

J. S. Famiglietti,[1] J. A. Devereaux,[1] C. A. Laymon,[2] T. Tsegaye,[3] P. R. Houser,[4] T. J. Jackson,[5] S. T. Graham,[1] M. Rodell,[1] and P. J. van Oevelen[6]

Abstract. Surface soil moisture content is highly variable in both space and time. While remote sensing provides an effective methodology for mapping surface moisture content over large areas, it averages within-pixel variability thereby masking the underlying heterogeneity observed at the land surface. This variability must be better understood in order to rigorously evaluate sensor performance and to enhance the utility of the larger-scale remotely sensed averages by quantifying the underlying variability that remote sensing cannot record explicitly. In support of the Southern Great Plains 1997 (SGP97) Hydrology Experiment (a surface soil moisture mapping mission conducted between June 18 and July 17, 1997, in central Oklahoma) an investigation was conducted to characterize soil moisture variability within remote sensing footprints (approximately 0.64 km^2) with more certainty than would be afforded with conventional gravimetric moisture content sampling. Nearly every day during the experiment period, portable impedance probes were used to intensively monitor volumetric moisture content in the 0- to 6-cm surface soil layer at six footprint-sized fields scattered over the SGP97 study area. A minimum of 49 daily moisture content measurements were made on most fields. Higher-resolution grid and transect data were also collected periodically. In total, more than 11,000 impedance probe measurements of volumetric moisture content were made at the six sites by over 35 SGP97 participants. The wide spatial distribution of the sites, combined with the intensive, near-daily monitoring, provided a unique opportunity (relative to previous smaller-scale and shorter-duration soil moisture studies) to characterize variations in surface moisture content over a range of wetness conditions. In this paper the range and temporal dynamics of the variability in moisture content within each of the six fields are described, as are general relationships between the variability and footprint-mean moisture content. Results indicate that distinct differences in mean moisture content between the six sites are consistent with variations in soil type, vegetation cover, and rainfall gradients. Within fields the standard deviation, coefficient of variation, skewness, and kurtosis increased with decreasing moisture content; the distribution of surface moisture content evolved from negatively skewed/nonnormal under very wet conditions, to normal in the midrange of mean moisture content, to positively skewed/nonnormal under dry conditions; and agricultural practices of row tilling and terracing were shown to exert a major control on observed moisture content variations. Results presented here can be utilized to better evaluate sensor performance, to extrapolate estimates of subgrid-scale variations in moisture content across the entire SGP97 region, and in the parameterization of soil moisture dynamics in hydrological and land surface models.

1. Introduction

Surface soil moisture content is an important hydrological variable which influences a wide range of interactions within Earth's climate system. For example, soil moisture stored near the land surface couples the land and the atmosphere by providing water vapor for precipitation through the process of evapotranspiration, by controlling the partitioning of net radiation into latent and sensible heat, and by providing thermal inertia to the climate system via heat storage and release from the vast terrestrial reservoirs. However, surface moisture content fluctuates at high spatial and temporal frequencies, which makes accurate characterization of its variability difficult over large areas. Such a characterization is required in order to better understand the mechanisms by which the land and the atmosphere interact and the degree to which these interactions drive and are driven by variations in weather and climate.

While remote sensing, especially L band (21-cm wavelength) passive microwave radiometry, offers the most promise for mapping surface (0–5 cm) soil moisture over large areas [*Jackson and Schmugge*, 1989; *Jackson and LeVine*, 1996], it averages soil moisture variability within sensor footprints thereby masking the underlying detail observed at the land surface. Because

[1]Department of Geological Sciences, University of Texas at Austin.
[2]Institute for Global Change Research and Education, Global Hydrology and Climate Center, Huntsville, Alabama.
[3]Department of Plant and Soil Science, Alabama A and M University, Normal.
[4]Hydrological Sciences Branch and Data Assimilation Office, NASA Goddard Space Flight Center, Greenbelt, Maryland.
[5]Hydrology Laboratory, Agricultural Research Service, U.S. Department of Agriculture, Beltsville, Maryland.
[6]Department of Water Resources, Wageningen Agricultural University, Wageningen, Netherlands.

Paper number 1999WR900047.
0043-1397/99/1999WR900047$09.00

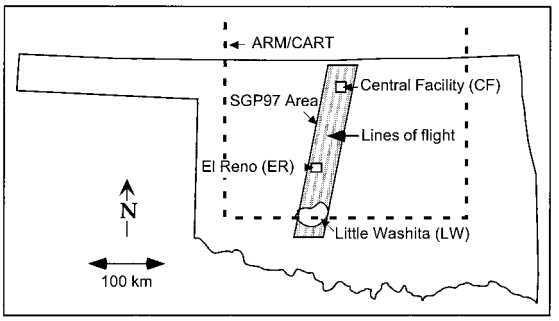

Figure 1. Location of Southern Great Plains 1997 (SGP97) Hydrology Experiment. Dashed line outlines Department of Energy Atmospheric Radiation Measurement Program/cloud and radiation test bed (ARM/CART) region. Solid line shows SGP97 study region. Ground truth and other data collection activities, including those described in this paper, were concentrated in the Little Washita watershed, the U.S. Department of Agriculture Agriculture Research Service Grazinglands Research Laboratory in El Reno, and the ARM/CART Central Facility.

many Earth system processes are nonlinearly dependent upon surface moisture content, this variability and hence the degree to which remote measurements reflect actual moisture conditions within footprints must be better understood in order to enable full utilization of the larger-scale remotely sensed averages by the Earth science community.

The purpose of this paper is to describe a field investigation of soil moisture variability within remote sensing footprints during the Southern Great Plains 1997 (SGP97) Hydrology Experiment. SGP97 was the largest airborne L band passive microwave mapping mission of surface soil moisture to date. Located in the 40-km by 250-km strip of central Oklahoma shown in Figure 1, soil moisture was mapped at a 0.8-km ground resolution nearly every day between June 18 and July 17, 1997. The area of the mapped region was an order of magnitude larger than in the previous experiment (Washita '92 [*Jackson and Levine*, 1996]) which utilized the same aircraft-based remote sensing instrument (the Electronically Scanned Thinned-Array Microwave Radiometer (ESTAR) [*LeVine et al.*, 1994]), and the duration of the experiment was 4 times greater. The objective of SGP97 was to demonstrate the potential of ESTAR for mapping surface soil moisture over large regions, with implications for the potential of a spaceborne *L* band passive microwave instrument to map surface soil moisture globally. A more detailed description of the experiment is provided by T. J. Jackson (Southern Great Plains 1997 (SGP97) Hydrology Experiment Plan, http://hydrolab.arsusda.gov/sgp97/, 1997).

Ground truth data in support of soil moisture remote sensing experiments have typically been collected using the gravimetric method. Such was the case during SGP97, in which field-mean soil moisture content was determined gravimetrically at 49 sites scattered over the mapped region. Thirty-five of these sites were 0.8-km by 0.8-km (the approximate size of the sensor footprint) winter wheat or rangeland fields typical of the region. In these fields, moisture content was sampled each day at 14 points. In the remaining 14 sites, which were smaller than the other 35 fields, nine soil moisture samples were collected each day. Note that the sampling time required by the gravimetric method, combined with the time required to travel to the 49 sites, limits the number of moisture content measurements that can be made on each field on each day.

Recent advances in impedance probe technology have resulted in the development of relatively inexpensive instruments capable of rapid volumetric moisture content determination. In our investigation, which was designed to complement the gravimetric ground truth data collection effort, portable impedance probes (see section 3 and Figure 2) were used to intensively monitor soil moisture content on six of the 35 winter wheat or rangeland fields. Volumetric moisture content in the 0- to 6-cm surface soil layer was measured nearly every day at 49 points on a 7 by 7 100-m grid at five of the six fields and at 27 points on a 3 by 8 100-m grid on the sixth field (see Figure 3). Higher-resolution grid and transect data were also collected periodically. In total, more than 11,000 impedance probe measurements of soil moisture were made at the six sites by over 35 SGP97 participants. Note that during the experiment, related studies of soil moisture variability within remote sensing foot-

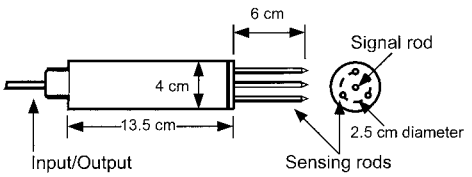

Figure 2. Soil moisture impedance probe.

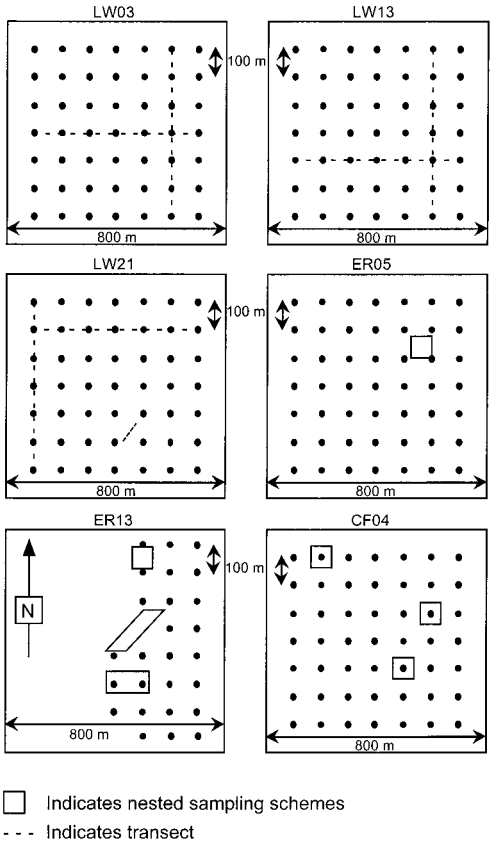

Figure 3. Soil moisture sampling plans at the six sites. Dots indicate measurement locations. Dashed lines show locations of higher-resolution transects. Boxes within fields show locations of higher-resolution grid sampling.

prints were simultaneously being conducted by other investigators on other fields within the SGP97 region. These activities and additional data sources are described by *Famiglietti* [1999].

Thus the rapid probe measurements provided a high-resolution sampling component that enabled a more accurate characterization of the mean and variability of surface soil moisture content within sensor footprints than would have been possible with the relatively small number of samples collected by the gravimetric method [*Bell et al*., 1980; *Owe et al*., 1982]. Additionally, the wide spatial distribution of the sites provided the opportunity to observe soil moisture variability over a range of wetness conditions resulting from regional rainfall gradients and local controls on surface drying. The combination of these two aspects of this study afforded a unique opportunity to observe and quantify the dynamics of surface moisture content variability that has not been possible in previous, smaller-scale and shorter-duration soil moisture studies (several of which are discussed in section 2).

In this paper the range and temporal dynamics of the variability in moisture content within each of the six fields are described, as are general relationships between the variability and field-mean moisture content. Specifically, the means and standard deviations versus time and the standard deviation, coefficient of variation, skewness, and kurtosis versus mean moisture content are presented for each field, and the time variation of frequency distributions and higher-resolution transect data are presented for selected fields and/or dates. By providing well-constrained estimates of the mean, higher-order statistics, and distributions of surface soil moisture within sensor footprints, our work will help quantify both the accuracy of ESTAR soil moisture estimates and the underlying variability that remote sensing cannot record explicitly. Estimates of higher-order statistical information will enable broader utilization of the ESTAR data since many Earth system processes are nonlinearly related to subgrid distributions of soil moisture. A thorough investigation of ESTAR performance, using both the impedance probe data and the gravimetric moisture content data, is the topic of current research and will be published separately at a later date.

Our study also represents an important step toward addressing the ground-based and remotely sensed sampling issues identified as imperative to soil moisture research by *Wei* [1995]. These include (1) characterizing the underlying spatial-temporal covariance structure of the soil moisture field being sampled, (2) quantifying the errors resulting from discrete, ground-based sampling schemes of these variable soil moisture fields, (3) quantifying the ability of remote sensing to provide accurate, integrated soil moisture of such variable fields at the footprint scale, and (4) characterizing the behavior of soil moisture variability across scales. This present study has important implications for issues 1 and 2 above. Ongoing research mentioned above, in which the impedance probe data are compared to the gravimetric ground truth data and to the ESTAR moisture content estimates, will provide insight into the third of these issues. Because our study has added a high-resolution component to the SGP97 ground truth data set, it will enable a more comprehensive study of the fourth issue.

2. Background

In this section, previous field investigations of surface soil moisture variability are reviewed. Studies included are those which have focused on moisture content variations in the near surface (0–15 cm) soil layer and which were conducted either in support of past soil moisture remote sensing experiments [e.g., *Rao and Ulaby*, 1977; *Bell et al*., 1980; *Owe et al*., 1982; *Charpentier and Groffman*, 1992] or at horizontal scales consistent with these past experiments [*Hills and Reynolds*, 1969; *Reynolds*, 1974; *Henninger et al*., 1976; *Hawley et al*., 1983; *Francis et al*., 1986; *Loague*, 1992; *Robinson and Dean*, 1993; *Nyberg*, 1996; *Famiglietti et al*., 1998]. Studies in which variations in surface moisture content have been characterized statistically are emphasized here. A detailed review of the environmental factors responsible for the observed variations is provided elsewhere [*Famiglietti et al*., 1998].

Because several hydrological, ecological, biogeochemical, and atmospheric processes are nonlinearly related to surface soil moisture, knowledge of its statistical distribution within remote sensing footprints would greatly increase the utility of remotely sensed soil moisture products within the Earth system science community. *Hills and Reynolds* [1969], *Bell et al*. [1980], *Hawley et al*. [1983], *Francis et al*. [1986], and *Nyberg* [1996] all found that surface soil moisture content was normally distributed within their study areas. *Loague* [1992] noted that surface moisture content sampled along linear transects was normally distributed, while that sampled on a grid was not. *Charpentier and Groffman* [1992] found that moisture content distributions observed within remote sensing footprints (66 m by 66 m) were often positively skewed, with low probabilities of being normal.

Several investigators have sought to identify relationships between the standard deviation or the coefficient of variation of moisture content and its mean value within an area. Because mean moisture content changes with time, such relationships can be used to determine changes in the number of samples required to estimate the mean moisture content within a specified limit of error [*Hills and Reynolds*, 1969; *Reynolds*, 1974; *Rao and Ulaby*, 1977; *Bell et al*., 1980; *Owe et al*., 1982], to estimate changes in the limit of error associated with a prescribed number of samples, to estimate the variability of surface moisture content within an area of land surface given its remotely sensed mean, and to infer changes in the accuracy and precision of remote sensing [*Charpentier and Groffman*, 1992]. *Hills and Reynolds* [1969], *Henninger et al*. [1976], *Bell et al*. [1980], *Robinson and Dean* [1993], and *Famiglietti et al*. [1998] all observed that the standard deviation of surface moisture content decreases as its mean decreases. *Owe et al*. [1982] found that the standard deviation peaks in the midrange of mean moisture content. *Hawley et al*. [1983] and *Charpentier and Groffman* [1992] found no systematic variation of the standard deviation with mean moisture content. *Bell et al*. [1980], *Owe et al*. [1982], and *Charpentier and Groffman* [1992] all reported a decrease in the coefficient of variation with increasing moisture content. *Charpentier and Groffman* [1992] suggested that under conditions of increased variance, remotely sensed footprint means would be less reflective of actual soil moisture conditions on the ground and that since the coefficient of variation increases with decreasing moisture content, soil moisture remote sensing will be more precise under wet conditions than dry.

3. Methods

A number of important constraints required consideration in the design of the experiment plan for this research. Since this study was a complementary investigation within SGP97, many of these constraints were dictated by the larger experi-

Table 1. Field Attributes

Site[a]	Location[b]	Cover Type[c]	Soil Type	Topography[d]	Comments[e]
LW03	584467, 3869166	rangeland	loamy sand	gently rolling	terracing
LW13	595701, 3864517	rangeland	loam	gently rolling	terracing
LW21	566047, 3863463	winter wheat	silty loam	flat	
ER05	587539, 3934392	rangeland	silty loam	gently rolling	terracing
ER13	585099, 3933578	winter wheat	silty loam	flat	
CF04	635121, 4053846	winter wheat	silty loam	flat	

[a]Site identifications are as follows: LW, Little Washita; ER, U.S. Department of Agriculture Agriculture Research Science Grazinglands Research Laboratory; CF, Atmospheric Radiation Measurement Program cloud and radiation test bed Central Facility. Last two digits indicate SGP97 ground truth field number.
[b]Universal transverse mercator coordinates of northeast corner of field. All fields are 800 m by 800 m and are aligned on a north-south grid.
[c]Effective cover type for most of the experiment was row-tilled bare soil for LW21 and ER13 and was wheat stubble for CF04. See Table 2 for cultivation dates.
[d]For simplicity we recognize two classes of topography: flat and gently rolling.
[e]Terracing refers to a common regional erosion control practice of building berms along terrain contours to inhibit downslope surface water flow.

ment. These included limitations with respect to site access, manpower, time available for sampling, and budget; a desire to reasonably limit travel time to sites and time in the field collecting data; and the large size of the SGP97 region. Given these constraints, the final plan, as outlined in sections 3.1–3.3, maximized the number of fields that could be sufficiently sampled on a daily basis, while providing an adequate distribution of study sites across the SGP97 experimental area.

3.1. Site Selection

Our six sites were a subset of the 49 sites which were selected as ground truth locations where soil moisture content was measured by the gravimetric method. These 49 sites were chosen such that the range of topographic, soil, and vegetation cover conditions found throughout the SGP97 region was well represented. Their selection was also influenced by important logistical issues such as the location of in situ or experiment-specific instrumentation, facility support, and site access. As such, the 49 sites for ground-based activities were concentrated in three primary locations: the Little Washita watershed, southwest of Chickasha (23 sites); the U.S. Department of Agriculture Agricultural Research Service Grazinglands Research Laboratory in El Reno (16 sites); and the Department of Energy Atmospheric Radiation Measurement Program cloud and radiation test bed (ARM CART) Central Facility, near Lamont (10 sites) (see Figure 1).

From these 49 sites, three fields were selected within the Little Washita (LW) watershed, two were selected at El Reno (ER), and one was selected at the ARM CART Central Facility (CF). These fields were identified during the experiment as LW03, LW13, LW21, ER05, ER13, and CF04, and they are listed in Table 1 along with their basic vegetative cover, soil, and topographic attributes. They represent typical combinations of cover and soil types found throughout the SGP97 region (e.g., winter wheat on silty loam and rangeland on loamy sand or loam), and their distribution across the experimental area maximized the likelihood that regional gradients in rainfall would be reflected in soil moisture observations.

3.2. Equipment

3.2.1. Soil moisture impedance probes. Central to the success of this investigation was the identification of a durable, portable, accurate, and affordable methodology for rapid measurement of surface soil moisture content. Given these requirements, we chose a new impedance probe, recently described by *Gaskin and Miller* [1996] and *Miller et al*. [1997] and now being produced commercially as the Theta Probe soil moisture sensor, type ML1, by Delta-T Devices of Cambridge, England. (The mention of product names does not constitute an endorsement of this product.)

The probe, shown in Figure 2, uses a simplified voltage standing wave method to determine the relative impedance of its sensing head (which consists of four sharpened 6-cm stainless steel wire rods) and thus the dielectric constant of the soil matrix and the volumetric water content of the soil. *Gaskin and Miller* [1996] and *Miller et al*. [1997] provide further details on probe operation. It is accurate to within ± 0.02 cm^3/cm^3 with site-specific calibration, and probe measurements of moisture content compare well with those of the neutron probe [*Gaskin and Miller*, 1996]. Site-specific calibration efforts by several of the coauthors yielded calibration curves similar to that of *Gaskin and Miller* [1996], so that the Gaskin and Miller calibration curve was adopted for use in this study.

The probe is compact, and it proved to be field durable in our study, though the 6-cm stainless steel wire rods tended to bend and break under the very dry conditions encountered in some fields. In most cases, however, bent or broken rods were easily repaired or replaced in the field. While several probes may have been used on each field (typically three or four for the duration of the experiment), comparisons done at each site showed that differences in probe responses were negligible.

3.2.2. Differential Global Positioning System (DGPS). Differential Global Positioning System was used to accurately geolocate sampling locations within fields and when real-time navigation was required in the field. DGPS functions by correcting for most of the natural and man-made errors that are a component of normal GPS measurements. Corrections are transmitted from a "reference" receiver, which is fixed in position, to the roving receivers in the field so that horizontal position can be determined to within 1–5 m.

Our DGPS system was composed of a 12-channel hand-held GPS receiver, a radio beacon receiver to receive the correction, a 2.6-m whip antenna, which was attached to the radio beacon receiver, and a 12-volt battery. In the field the radio beacon receiver, the whip antenna, and the battery were carried in a small backpack. The correction signal was transmitted by radio beacon from a reference station in Sallisaw, Okla-

homa, which is part of a network maintained by the U.S. Coast Guard for navigational purposes. The system described above was relatively inexpensive and field durable and performed well for the purposes of our experiment.

3.3. Sampling Plan

Volumetric moisture content in the 0- to 6-cm surface soil layer was measured nearly every day at 49 points on a 7 by 7 100-m grid at five of the six fields sites (LW03, LW13, LW21, ER05, and CF04) and at 27 points on a 3 by 8 100-m grid on the sixth field (ER13, see Figure 3). Additionally, higher-resolution data were collected at several of the sites. These included 25-m north-south and east-west transects (LW03 and LW21), higher-resolution transects along which samples were collected at distinct intervals of variable length (e.g., at tops and bottoms of tilled soil rows (LW21) or terraced hillslopes (LW13)), and on higher-resolution grids (ER05, ER13, and CF04). Table 2 lists the additional data collected at each of the six sites.

Once sampling grids were established at each of the six fields, moisture content sampling was conducted on each day possible. Sampling was suspended during rain events or when agricultural activity (e.g., cultivating and fertilizer or pesticide spreading) posed a significant safety concern. In general, two 2-person teams were assigned to each field. One person operated the DGPS and recorded the data, while the second person sampled moisture content with the impedance probe. Sampling was routinely conducted between the hours of 1 and 3 P.M. CST. The dates on which sampling was conducted are listed in Table 2 for each field along with a statistical summary of the daily measurements. In total, more than 11,000 impedance probe measurements of soil moisture were made on the six fields during the course of the experiment. All data are available through the NASA Goddard Distributed Active Archive Center at http://daac.gsfc.nasa.gov.

4. Results

4.1. Mean Moisture Content

Figure 4 shows the time series of precipitation and the mean and standard deviation of surface moisture content for each of the six fields. The mean moisture content responds predictably to rainfall, increasing after storm events and decreasing thereafter. The El Reno and Central Facility fields were often wetter than those in the Little Washita watershed, in particular during the second and third weeks of the experiment, owing to the greater depth of precipitation falling in the central and northern parts of the study region. Field ER05 was the wettest site, with mean moisture content values ranging between 0.48 cm^3/cm^3 and 0.28 cm^3/cm^3. The driest site was LW03, in which the mean moisture content varied between 0.22 cm^3/cm^3 and 0.05 cm^3/cm^3.

Close inspection of Figure 4 and Table 2 reveals distinct differences in field-mean moisture content resulting from differences in soil types, vegetation cover, and rainfall gradients. For example, fields LW03 and LW13 are both covered by rangeland vegetation and received similar amounts of rainfall during the study period. However, the more sandy soil at LW03 resulted in a lower mean moisture content than at LW13 on all but one day. Fields ER05 and ER13 received comparable amounts of precipitation during the experiment and differed primarily in their type of vegetation cover. The winter wheat grown in ER13 was harvested early in the experiment so that its effective cover type was bare soil for most of the study period. Comparing field-mean moisture contents for the two fields shows that the bare field (ER13) was consistently drier than its rangeland neighbor (ER05). Finally, differences in mean moisture content due to differences in rainfall are evident from comparing field LW21 with ER13: both are winter wheat fields on silty loam soil which differed primarily in the depth of precipitation falling during the course of the experiment. As mentioned above, during the second and third weeks of the experiment, more precipitation fell over the central (ER) and northern (CF) sites, and thus field-mean moisture contents at ER13 were much greater than those at LW21 during this phase of the study.

4.2. Standard Deviation and Coefficient of Variation of Moisture Content

Figure 4 and Table 2 also show that observed standard deviations of moisture content within each field varied between upper and lower limits of 0.09 cm^3/cm^3 and 0.01 cm^3/cm^3, respectively. These data further suggested potential relationships between the standard deviation of moisture content and its mean value. Figure 5a shows the standard deviation of moisture content within each field versus its mean value, for each of the six fields, for each day on which data were obtained. Although there is a good deal of scatter in this relationship, it indicates a general decrease in the standard deviation or absolute variability, with increasing mean moisture content. Note that this result is in contrast with previous findings by *Hills and Reynolds* [1969], *Henninger et al*. [1976], *Bell et al*. [1980], *Robinson and Dean* [1993], and *Famiglietti et al*. [1998], all of whom found an increase in the standard deviation with increasing moisture content.

The relationship between relative variability, as measured by the coefficient of variation, and the mean moisture content is shown in Figure 5b. Relative variability clearly decreases with increasing moisture content, which is consistent with the findings of earlier studies by *Bell et al*. [1980], *Owe et al*. [1982], and *Charpentier and Groffman* [1992]. The observed decrease is largely controlled by increasing mean moisture content rather than decreasing standard deviation, since the range of the observed mean moisture content is nearly 6 times greater than the range of the standard deviation.

4.3. Distributions, Skewness, and Kurtosis

Frequency distributions of surface moisture content are shown in Figure 6 for each field on selected days during drydown sequences within the study period. Distinct differences are evident between the drier fields within the Little Washita watershed and the wetter fields at the El Reno and Central Facility locations. In the Little Washita fields the distributions appear normal following rain events but become positively skewed as the soil dries with increasing time into the interstorm period. This observation is supported by the results of normality testing with the Shapiro-Wilk statistic, which indicated (Table 2) that all of the LW03 distributions shown in Figure 6, the June 28, July 1, and July 3 distributions at LW13 and the July 6 and July 8 distributions at LW21, have low probabilities of being normal. It is further supported by the increase in skewness reported in Table 2.

The heavier rainfall in the central and northern parts of the SGP97 study region provided an opportunity to observe surface moisture content distributions under wetter conditions than those observed in the Little Washita watershed. The high-

Table 2. Summary of Field Data

Site	Number of Samples	Date	Mean	Standard Deviation	Coefficient of Variation	Kurtosis	Skewness	Normality (Shapiro-Wilk)	Comments
LW03	49	June 19, 1997	0.167	0.0760	0.456	0.2537	0.4478	normal	
	49	June 20, 1997	0.145	0.0879	0.606	0.5990	1.0709	nonnormal	
	49	June 21, 1997	0.141	0.0869	0.615	0.3211	0.8080	nonnormal	
	49	June 22, 1997	0.123	0.0833	0.676	0.2953	0.9206	nonnormal	
	0	June 23, 1997							
	49	June 24, 1997	0.210	0.0715	0.340	0.0089	0.6960	normal	
	49	June 25, 1997	0.187	0.0709	0.379	0.0245	0.6268	nonnormal	
	49	June 26, 1997	0.221	0.0686	0.310	−0.1674	0.8143	nonnormal	
	49	June 27, 1997	0.200	0.0671	0.335	−0.1466	0.9463	nonnormal	
	49	June 28, 1997	0.195	0.0675	0.346	−0.0818	0.7899	nonnormal	
	49	June 29, 1997	0.170	0.0707	0.415	0.3479	1.0464	nonnormal	
	49	June 30, 1997	0.143	0.0763	0.532	0.4958	1.0083	nonnormal	
	49	July 1, 1997	0.130	0.0812	0.624	1.6867	1.4462	nonnormal	
	49	July 2, 1997	0.087	0.0941	1.085	1.7331	1.2829	nonnormal	
	49	July 3, 1997	0.087	0.0798	0.917	2.7847	1.6701	nonnormal	
	0	July 4, 1997							
	49	July 5, 1997	0.088	0.0619	0.705	3.7697	1.9043	nonnormal	
	49	July 6, 1997	0.085	0.0758	0.894	3.5186	1.9705	nonnormal	
	49	July 7, 1997	0.072	0.0566	0.783	1.8989	1.5098	nonnormal	
	49	July 8, 1997	0.064	0.0604	0.942	5.2881	2.1290	nonnormal	
	49	July 9, 1997	0.053	0.0575	1.092	4.6839	2.1416	nonnormal	
	0	July 10, 1997							
	49	July 11, 1997	0.193	0.0560	0.291	0.1384	0.8319	nonnormal	
	0	July 12, 1997							
	49	July 13, 1997	0.132	0.0411	0.311	1.2795	1.0666	nonnormal	
	49	July 14, 1997	0.127	0.0504	0.396	2.7157	1.4247	nonnormal	
	0	July 15, 1997							
	49	July 16, 1997	0.167	0.0530	0.319	1.0318	1.0338	nonnormal	
LW13	49	June 19, 1997	0.285	0.0519	0.182	−0.0191	−0.0064	normal	
	49	June 20, 1997	0.262	0.0567	0.217	0.0551	−0.0002	normal	
	49	June 21, 1997	0.250	0.0680	0.272	0.6427	−0.0406	normal	T
	49	June 22, 1997	0.220	0.0701	0.318	−0.0372	0.2597	normal	
	0	June 23, 1997							
	49	June 24, 1997	0.264	0.0521	0.197	0.4627	0.3968	normal	
	49	June 25, 1997	0.237	0.0644	0.272	−0.1179	0.4699	normal	T
	49	June 26, 1997	0.262	0.0609	0.233	−0.3286	0.4387	normal	
	49	June 27, 1997	0.192	0.0938	0.489	−0.7571	−0.0382	normal	T
	49	June 28, 1997	0.204	0.0660	0.324	0.7731	0.9631	nonnormal	
	49	June 29, 1997	0.183	0.0651	0.355	1.6819	1.2926	nonnormal	
	0	June 30, 1997							
	49	July 1, 1997	0.166	0.0680	0.411	1.3125	1.0591	nonnormal	
	49	July 2, 1997	0.151	0.0660	0.437	1.9573	0.9715	nonnormal	
	49	July 3, 1997	0.143	0.0594	0.415	3.7281	1.8936	nonnormal	
	49	July 4, 1997	0.216	0.0472	0.219	3.6203	0.5067	normal	
	49	July 5, 1997	0.200	0.0424	0.212	2.3393	1.1398	nonnormal	
	49	July 6, 1997	0.174	0.0506	0.290	5.8897	1.9721	nonnormal	T
	49	July 7, 1997	0.155	0.0426	0.275	3.3719	1.1909	nonnormal	T
	24	July 8, 1997	0.152	0.0526	0.346	1.6345	1.4985	nonnormal	T
	49	July 9, 1997	0.136	0.0409	0.300	7.7329	2.0698	nonnormal	T
	0	July 10, 1997							
	49	July 11, 1997	0.325	0.0270	0.083	1.3779	0.3835	normal	T
	49	July 12, 1997	0.279	0.0259	0.093	3.4539	1.1912	nonnormal	T
	49	July 13, 1997	0.247	0.0325	0.132	0.1604	−0.3337	normal	T
	49	July 14, 1997	0.217	0.0362	0.167	0.2394	0.0670	normal	T
	49	July 15, 1997	0.187	0.0358	0.192	−0.5889	0.1325	normal	T
	49	July 16, 1997	0.182	0.0413	0.227	−0.5382	0.0449	normal	
LW21	49	June 22, 1997	0.244	0.0421	0.173	−0.1018	0.3452	normal	S
	0	June 23, 1997							S
	49	June 24, 1997	0.259	0.0418	0.162	−0.7019	0.1484	normal	S
	0	June 25, 1997							S
	49	June 26, 1997	0.228	0.0556	0.244	0.2371	0.0170	normal	S
	0	June 27, 1997							B
	49	June 28, 1997	0.238	0.0584	0.245	0.3253	0.0209	normal	B, T
	49	June 29, 1997	0.213	0.0632	0.297	−0.3257	0.3017	normal	B, T
	49	June 30, 1997	0.181	0.0781	0.431	−0.6318	0.0607	normal	B, T
	49	July 1, 1997	0.156	0.0664	0.426	−0.7179	−0.0472	normal	B, T
	49	July 2, 1997	0.148	0.0692	0.467	0.4532	0.4545	normal	B, T
	49	July 3, 1997	0.113	0.0768	0.680	−0.9288	0.0326	nonnormal	B, T
	0	July 4, 1997							B
	49	July 6, 1997	0.105	0.0768	0.730	−0.6346	0.3136	nonnormal	B
	49	July 7, 1997	0.098	0.0689	0.701	−0.7392	0.0227	nonnormal	B
	49	July 8, 1997	0.093	0.0754	0.812	−0.2188	0.5126	nonnormal	B, T

Table 2. (continued)

Site	Number of Samples	Date	Mean	Standard Deviation	Coefficient of Variation	Kurtosis	Skewness	Normality (Shapiro-Wilk)	Comments
LW21	0	July 9, 1997							B
	0	July 10, 1997							B
	49	July 11, 1997	0.270	0.0608	0.225	0.0911	−0.3691	normal	B, T
	49	July 12, 1997	0.233	0.0614	0.264	1.7538	−0.8912	nonnormal	B, T
	49	July 13, 1997	0.204	0.0648	0.317	−0.3441	−0.1514	normal	B, T
	49	July 14, 1997	0.189	0.0697	0.369	−0.3399	−0.2819	normal	B, T
	0	July 15, 1997							B
	49	July 16, 1997	0.190	0.0460	0.242	−0.7672	0.1914	normal	B
ER05	49	June 19, 1997	0.482	0.0472	0.098	0.4973	−0.8948	nonnormal	
	49	June 20, 1997	0.366	0.0427	0.117	−0.5023	−0.3897	normal	
	49	June 21, 1997	0.332	0.0561	0.169	0.2083	−0.5043	normal	
	49	June 22, 1997	0.351	0.0744	0.212	−0.6027	0.0108	normal	
	0	June 23, 1997							
	49	June 24, 1997	0.398	0.0810	0.204	−0.4678	−0.1708	normal	
	49	June 25, 1997	0.322	0.0665	0.207	−0.0054	−0.6070	normal	
	0	June 26, 1997							
	49	June 27, 1997	0.365	0.0334	0.092	−0.5863	−0.3114	normal	3R, N
	0	June 28, 1997							
	49	June 29, 1997	0.394	0.0403	0.102	0.0492	0.6188	normal	3R, N
	0	June 30, 1997							
	49	July 1, 1997	0.363	0.0406	0.112	−0.5596	−0.2482	normal	3R
	49	July 2, 1997	0.360	0.0555	0.154	−0.4241	−0.3377	normal	3R, N
	49	July 3, 1997	0.322	0.0565	0.175	−0.2170	−0.0345	normal	3R
	0	July 4, 1997							
	49	July 5, 1997	0.347	0.0290	0.084	0.2926	0.0515	normal	3R
	49	July 6, 1997	0.345	0.0417	0.121	−0.5693	0.0577	normal	3R
	49	July 7, 1997	0.316	0.0538	0.170	−0.3266	0.2616	normal	3R
	49	July 8, 1997	0.355	0.0935	0.264	−0.6941	−0.1680	normal	3R, N
	0	July 9, 1997							
	49	July 10, 1997	0.285	0.0561	0.197	0.4985	0.6597	normal	3R
	0	July 11, 1997							
	49	July 12, 1997	0.342	0.0711	0.208	0.0991	−0.2180	normal	3R, N
	46	July 13, 1997	0.301	0.0511	0.170	−0.8381	−0.0702	normal	3R, N
	46	July 14, 1997	0.285	0.0514	0.181	−1.0634	0.1192	normal	3R
	49	July 15, 1997	0.278	0.0522	0.188	0.3775	−0.1932	normal	3R
ER13	27	June 19, 1997	0.337	0.035	0.105	−0.4021	0.3370	normal	B
	27	June 20, 1997	0.262	0.074	0.281	1.1299	1.1991	nonnormal	B
	27	June 21, 1997	0.274	0.070	0.257	1.4851	0.9528	normal	B
	27	June 22, 1997	0.227	0.067	0.295	0.1560	0.9343	nonnormal	B
	0	June 23, 1997							B
	27	June 24, 1997	0.280	0.086	0.308	−0.5542	−0.1543	normal	B
	27	June 25, 1997	0.262	0.075	0.286	−1.2977	−0.2076	normal	B
	0	June 26, 1997							B
	27	June 27, 1997	0.288	0.062	0.214	−0.1396	−0.3381	normal	B, 3R
	0	June 28, 1997							B
	27	June 29, 1997	0.390	0.050	0.129	0.5298	0.2834	normal	B, 3R
	27	June 30, 1997	0.342	0.065	0.191	−0.2411	0.3671	normal	B, 3R
	27	July 1, 1997	0.275	0.055	0.202	2.0413	1.3148	nonnormal	B, 3R
	27	July 2, 1997	0.264	0.045	0.171	0.6633	0.5534	normal	B, 3R
	27	July 3, 1997	0.245	0.042	0.173	0.6486	0.8328	normal	B, 3R
	0	July 4, 1997							B
	27	July 5, 1997	0.330	0.033	0.100	−0.0767	−0.2167	normal	B, 3R, N
	27	July 6, 1997	0.252	0.039	0.153	0.2010	−0.0978	normal	B, 3R, N
	27	July 7, 1997	0.253	0.041	0.161	−0.7346	0.1949	normal	B, 3R, N
	27	July 8, 1997	0.235	0.035	0.149	2.4529	1.1855	nonnormal	B, 3R, N
	27	July 9, 1997	0.219	0.035	0.158	3.4689	1.5173	nonnormal	B, 3R, N
	8	July 10, 1997	0.211	0.014	0.068	−0.9006	−0.1351	normal	B, 3R
	27	July 11, 1997	0.244	0.048	0.196	0.0766	−0.0271	normal	B, 3R, N
	27	July 12, 1997	0.201	0.041	0.203	0.9499	0.3123	normal	B, 3R, N
	27	July 13, 1997	0.186	0.053	0.285	−0.7109	0.2074	normal	B, 3R, N
	27	July 14, 1997	0.177	0.048	0.272	−0.9807	−0.0993	normal	B, 3R, N
	27	July 15, 1997	0.249	0.031	0.123	1.2103	0.4027	normal	B, 3R, N
CF04	27	June 21, 1997	0.242	0.0543	0.225	1.5320	−1.0917	nonnormal	S
	48	June 22, 1997	0.237	0.0578	0.243	−0.0786	0.0339	normal	S
	49	June 23, 1997	0.270	0.0585	0.216	−0.3741	0.0492	normal	S
	49	June 24, 1997	0.237	0.0557	0.235	0.2053	0.4712	normal	S
	49	June 25, 1997	0.218	0.0620	0.284	1.1577	0.0789	normal	S
	49	June 26, 1997	0.389	0.0384	0.099	2.6449	−0.1224	normal	S
	20	June 27, 1997	0.352	0.0414	0.117	−0.0903	−0.3735	normal	S
	49	June 28, 1997	0.337	0.0443	0.131	−0.2009	−0.2231	normal	S, N
	49	June 29, 1997	0.356	0.0350	0.098	1.1502	−0.6803	normal	S
	49	June 30, 1997	0.379	0.0324	0.085	2.2769	−1.0645	nonnormal	S

Table 2. (continued)

Site	Number of Samples	Date	Mean	Standard Deviation	Coefficient of Variation	Kurtosis	Skewness	Normality (Shapiro-Wilk)	Comments
Cf04	0	July 1, 1997							S
	45	July 2, 1997	0.318	0.0421	0.133	0.5703	−0.3428	normal	S
	28	July 3, 1997	0.276	0.0618	0.224	0.8637	−0.0493	normal	S
	49	July 4, 1997	0.270	0.0537	0.199	−0.3458	−0.0169	normal	S
	47	July 5, 1997	0.252	0.0506	0.201	−0.6085	0.1017	normal	S, N
	49	July 6, 1997	0.256	0.0682	0.267	0.2928	0.0951	normal	S
	49	July 7, 1997	0.224	0.0708	0.316	−0.3942	0.4041	normal	S
	49	July 8, 1997	0.218	0.0683	0.314	1.3084	0.6506	normal	S, N
	49	July 9, 1997	0.191	0.0778	0.407	1.4174	1.0087	nonnormal	S, N
	33	July 10, 1997	0.192	0.0758	0.395	1.5476	0.9738	normal	S
	41	July 11, 1997	0.321	0.0371	0.115	6.2356	−1.9825	nonnormal	S
	48	July 12, 1997	0.292	0.0557	0.191	1.6840	−0.7909	normal	S
	49	July 13, 1997	0.266	0.0553	0.208	1.3365	−0.0651	normal	D
	21	July 14, 1997	0.200	0.0719	0.359	−0.1587	0.1413	normal	D

Abbreviations are as follows: 3R, three readings taken at each point, only the first used in the calculations in this paper; N, nested-scale sampling taken; T, transect data taken; S, wheat stubble; B, row tilled/bare soil; and D, disk cultivated/bare soil (not row tilled). All data available at http://daac.gsfc.nasa.gov.

est daily value of mean moisture content at any of the six fields was observed on June 19 at ER05. Figure 6 and Table 2 show that the corresponding moisture content distribution under these very wet conditions (0.48 cm^3/cm^3 mean moisture content) was negatively skewed and was not normal. As the soil dried in the days following, positive skewness increased and the distributions tended toward normalcy. The distributions observed at ER13 remained normal for the interstorm period shown in Figure 6, and as in the case of the other fields shown in Figure 6, positive skewness increased as the soil dried. The heavy rains of June 26 and June 29 at CF04 and the 11-day dry-down period which followed allowed for direct observation of the temporal dynamics of a surface moisture content distribution during a relatively long interstorm period, in which moisture conditions changed from very wet to very dry. Though not visually apparent in Figure 6, Table 2 shows that the distribution began the drying cycle as negatively skewed and nonnormal. Then, Figure 6 and Table 2 clearly show that the distribution evolves to normal on July 2 and 7 and to positively skewed and nonnormal on July 9.

Figure 7a shows skewness versus mean moisture content for each field on each day that data were collected. Combining

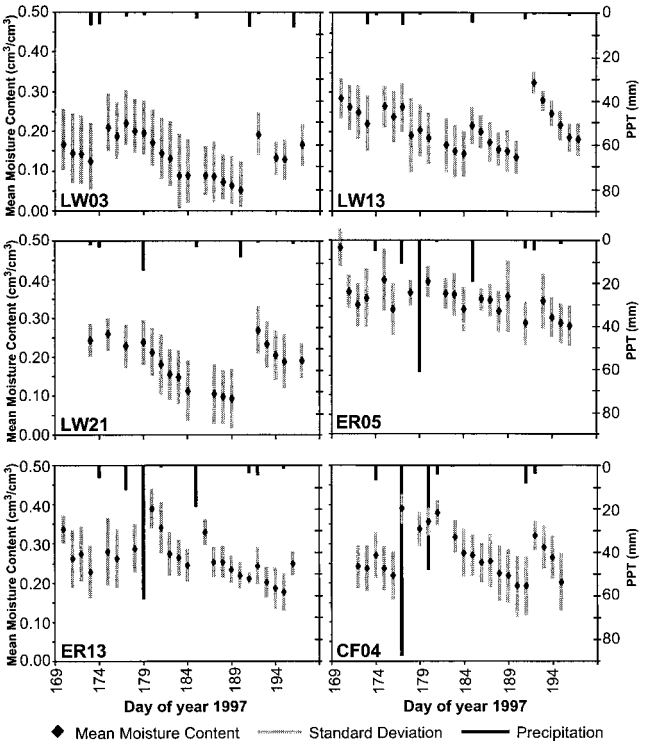

Figure 4. Mean (cm^3/cm^3) and standard deviation (cm^3/cm^3) of moisture content versus day of year (DOY) for the six sites. Also shown is daily precipitation depth (millimeters). DOY 169 is June 18.

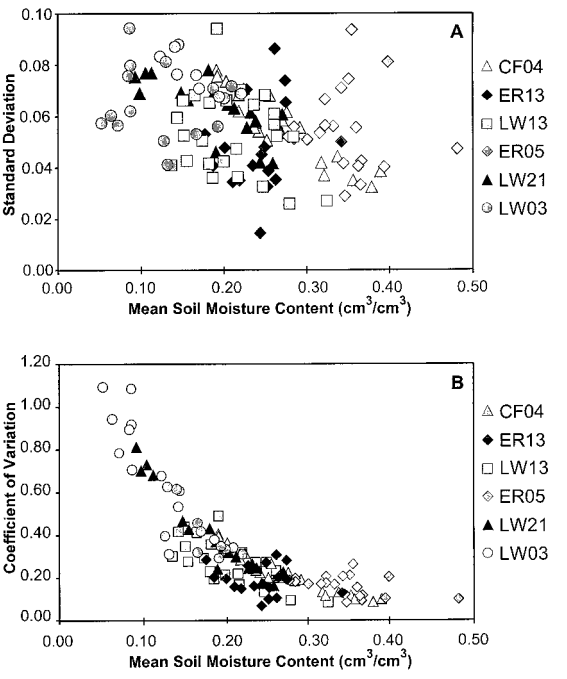

Figure 5. (a) Standard deviation (cm^3/cm^3) of moisture content versus mean moisture content (cm^3/cm^3) for the six sites. Despite the scatter (r^2 for linear regression is 0.2 and $\alpha = 0.05$) a general trend of decreasing standard deviation with increasing mean moisture content is apparent. (b) Coefficient of variation versus mean moisture content (cm^3/cm^3) for the six sites.

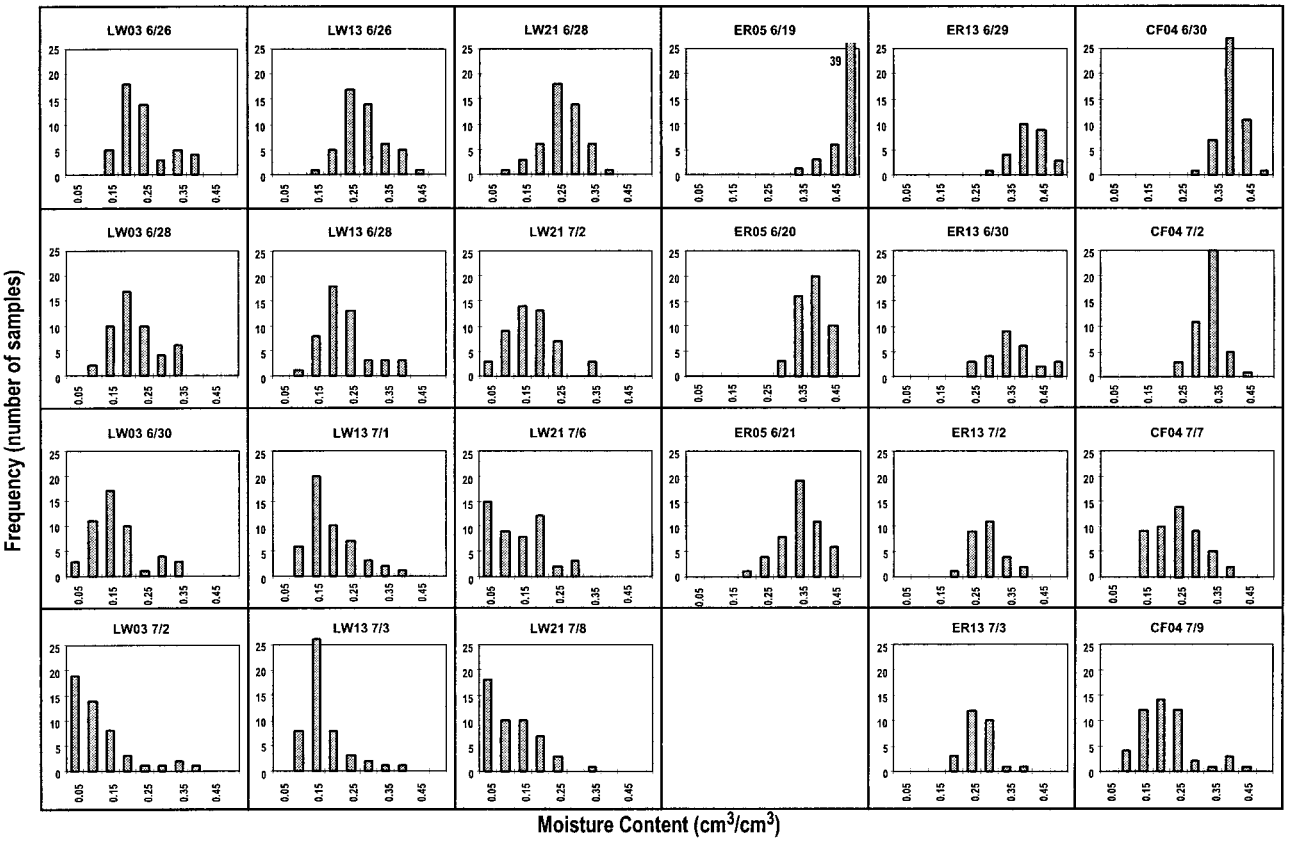

Figure 6. Frequency distributions of surface moisture content for the six sites on selected dates during dry-down periods.

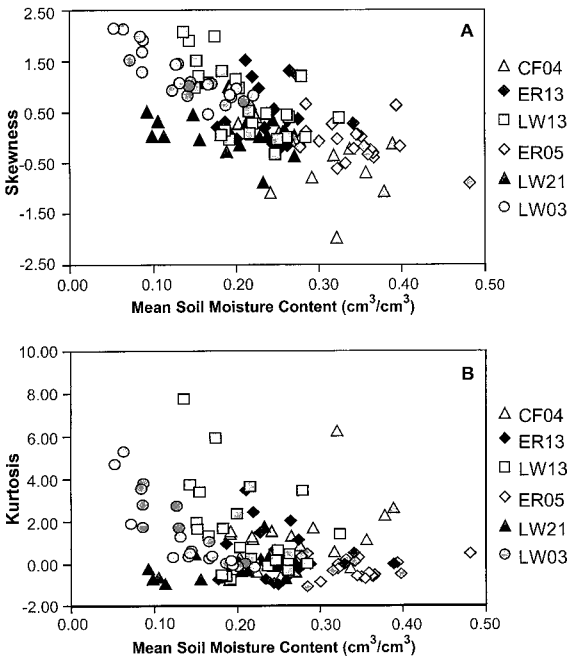

Figure 7. (a) Skewness versus mean moisture content (cm^3/cm^3) for the six sites. Despite the scatter (r^2 for linear regression is 0.42 and $\alpha = 0.05$) a general trend of decreasing skewness with increasing mean moisture content is apparent. (b) Kurtosis versus mean moisture content (cm^3/cm^3) for the six sites.

Figure 7 with Table 2 and visual inspection of all the daily distributions for all fields confirms the general trends outlined above, including increasing positive skewness with decreasing mean moisture content, negatively skewed/nonnormal or normal distributions under the wettest field conditions, normal distributions in the midrange of mean moisture content, and positively skewed/nonnormal distributions under the driest field conditions. Of the 63 daily moisture content distributions analyzed for the wetter ER05, ER13, and CF04 fields, 53 were normal according to the Shapiro-Wilk statistic. Although normal, 27 of the 53 distributions had negative values of skewness. Four of the 10 nonnormal distributions were negatively skewed and were observed following rain events, and three of the four occurred under some of the wettest conditions encountered during the study period: ER05 on June 19 and CF04 on June 26, June 30, and July 11. The remaining six were positively skewed and were associated with progressive soil drying during interstorm periods.

In contrast, of the 65 daily moisture content distributions analyzed for the drier LW03, LW13, and LW21 fields, only 28 were normal, and 21 of these had positive values of skewness. Nearly all of the remaining 37 nonnormal distributions were positively skewed and occurred later in interstorm periods with progressive drying of the soil at times when the Little Washita fields were the driest in the study region. In fact, most of these were observed on the driest field in the study, LW03, in which surface moisture content distributions were positively skewed on 21 of 23 days.

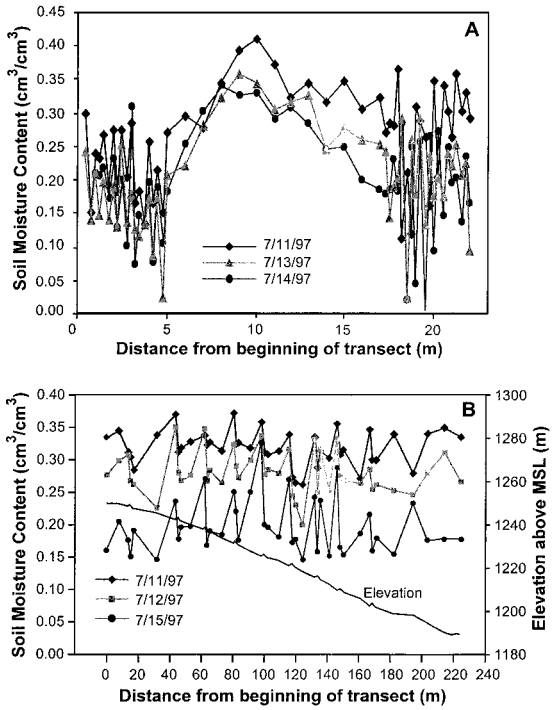

Figure 8. Moisture content (cm^3/cm^3) versus distance along transect for three dates at (a) LW21 and (b) LW13.

Kurtosis versus mean moisture content is shown in Figure 7b for all six fields for all days on which data were collected. Despite the scatter, Figure 7b suggests that kurtosis increases with decreasing moisture content. This relationship is strongest on the driest field, LW03, while kurtosis values for the wettest field, ER05, are clustered around zero. Hence the behavior of the kurtosis is consistent with the observed dynamics of moisture content distributions described above: kurtosis values near zero would be expected if normal distributions occurred under wetter conditions, and higher values would be expected if skewed distributions occurred under drier conditions. It is worth noting further that Figure 7b hints at a possible U-shaped kurtosis-mean moisture content relationship, with kurtosis increasing with increasing mean moisture content on the wettest fields (ER05 and CF04). A U-shaped relationship is also consistent with the general picture outlined above, as kurtosis would be expected to increase under the very wettest conditions when more of the moisture content distribution falls in the high range of soil wetness.

Several earlier field studies have noted that surface soil moisture content is often normally distributed [*Hills and Reynolds*, 1969; *Bell et al*., 1980; *Hawley et al*., 1983; *Francis et al*., 1986; *Nyberg*, 1996], and *Charpentier and Groffman* [1992] reported that the distributions were often positively skewed. However, to our knowledge, no previous field studies of soil moisture variability have documented a progressive change in skewness and kurtosis as a function of mean moisture content and the resulting changes in the form of moisture content distributions, from negatively skewed/nonnormal, to normal, to positively skewed/nonnormal, with continued soil drying during interstorm periods. This progressive evolution seems intuitive because soil moisture distributions are bounded at the upper and lower ends of the wetness range by porosity and a zero (or residual) value of moisture content, respectively. It is likely that previous field studies have been too limited in duration, area, and spatial-temporal sampling frequencies to observe these dynamics over the full range of soil wetness conditions. We will return to this topic in section 5.

4.4. Higher Spatial Resolution Sampling Activities

Higher-resolution moisture content sampling was conducted at each field on selected days when time, weather, and resources permitted. Though not a comprehensive effort, these additional surveys provided insight into the sources of the variability in surface moisture content described in previous sections. A summary of these auxiliary data is provided in Table 2. Results from two of these efforts, that is, transect studies at LW21 and LW13, are described below. Of particular interest in these two examples was the role of terracing and row tilling, two agricultural practices that are widespread throughout the SGP97 region and which have the potential to greatly alter the spatial distribution of surface soil moisture. Analysis of the higher-resolution data sets collected at the other fields is being pursued by several of the individual coauthors and will be published separately.

Field LW21, like the majority of the winter wheat fields in the SGP97 region, was harvested, disk cultivated, and row tilled early in the experiment period. Hence most winter wheat fields in the area were actually bare soil tilled into characteristic rows of ridges and furrows. Ridges were typically spaced 50 cm apart and measured 25 cm in height from furrow bottoms. In order to better understand the influence of the ridge-furrow microtopography on variability in surface moisture content, a short, 25-m transect (see Figure 3) was oriented perpendicular to the ridge-furrow rows, and moisture content was sampled at the top of each ridge and the bottom of each furrow. A dry creek bed was located in the middle of the transect, in which moisture content was sampled at 1-m intervals. In total, 50 measurements were made along the transect on 4 days (July 11–14) during a brief dry-down period in the last week of the experiment.

The influence of both agricultural activities and natural topography on moisture content variability are evident in the LW21 transect results shown in Figure 8a. The parallel ridges and furrows on either side of the dry creek bed yielded high-frequency variations in surface moisture content, with high values of moisture content found in the furrows and lower values found on the tops of ridges. In some cases, moisture content measured at adjacent ridges and furrows varied by as much as an order of magnitude (e.g., July 13 and 14 at 18 m). In the center of the transect along the dry creek bed, moisture content varied systematically with relative elevation, increasing along one side of the channel, peaking in the center, and decreasing along the other side. On each day the highest value of moisture content was located at or near the center of the creek bed, and the lowest value was found in a furrow. Figure 8a shows that the general features described above persisted as the transect dried down on July 13 and 14.

A second agricultural practice common to the region is terracing (particularly in the hillier rangeland fields) in which berms are constructed along hillslope contours to impede surface water flow for erosion control purposes. In order to better characterize the influence of terracing on variations in surface moisture content, a north-south and an east-west transect were established at LW13 (see Figure 3), both of which crossed several berms. Berms were spaced roughly 20 m apart, and moisture content measurements were made just above, on top

of, and just below each berm. Moisture content measurements were made at 7-m intervals between berms on the north-south transect and just once on the east-west transect. Table 2 lists the dates on which these transect data were collected.

Results for the 225-m east-west transect are shown in Figure 8b for 3 days (July 11, 12, and 15) during a brief interstorm period that occurred in the last week of the experiment. Also shown are the elevations of the 42 sampling locations along the transect. It is evident from Figure 8b that there is no correlation between surface moisture content and the significant downslope decrease in elevation. Rather, the most striking feature apparent in Figure 8b is that the presence of berms controls variability in surface moisture content along the transect: on each day, moisture content is consistently highest above each berm. Similar patterns were observed along the 230-m north-south transect (not shown).

5. Discussion

In this section the environmental factors responsible for the observed variations in surface moisture content, both within and between the six sites, are briefly discussed, as are the implications for this work with respect to understanding ESTAR accuracy, enhancing the utility of the SGP97 remotely sensed soil moisture imagery, and the parameterization of soil moisture dynamics in land surface models.

5.1. Environmental Controls on Soil Moisture Variability

Although the primary emphasis of this study was on the statistical characterization of variations in surface moisture content rather than on a detailed investigation of the responsible land surface properties and environmental processes, at least two aspects of the previously presented work warrant further discussion in this regard. First is the degree to which variations in soil type, vegetation cover, and rainfall gradients influenced variations in the mean moisture content between the six fields (see Figure 4). The distinct differences apparent in Figure 4 suggest that variations in surface moisture content due to large-scale variations in these controls should be readily detectable in the 0.8-km remotely sensed soil moisture data and as such should serve as a qualitative check on ESTAR performance. Higher-resolution results from the previous Washita '92 experiment [*Jackson and Levine*, 1996] suggest that this will, in fact, be the case.

A second point for discussion is the factors responsible for the observed moisture content variability within fields and, in particular, the evolution of moisture content distributions during the transition from wet to dry conditions. While a comprehensive study of the influence of within-field variations in process controls (e.g., topographic attributes, soil texture, vegetation cover, and precipitation) was not plausible in the context of this large-scale experiment, Figure 8 suggests that the widespread agricultural practices of row tilling and terracing played a major role in controlling subfootprint-scale soil moisture variability during the period of observation. Figure 8 (and similar transect results not shown) indicates further that their influence was continuous through interstorm periods and hence not limited to wet or dry conditions.

Row tilling and terracing influence the distribution of surface moisture content by imposing unnatural microtopographic (ridge-furrow rows on the LW21 and ER13 winter wheat fields and regularly spaced berms on the LW03, LW13, and ER05 rangeland fields) and porosity (tilled ridges on winter wheat fields were openly porous) structures on the six fields. Compaction due to grazing and agricultural equipment traffic was another factor that affected both soil structure and created topographic depressions. Under wet conditions, water drained rapidly from plowed ridges on the winter wheat fields and tended to accumulate in microtopographic lows in all fields (furrows on the winter wheat fields, behind berms on the rangeland fields, and in compacted areas on both field types). Together these variations in porosity and microtopography jointly controlled the distribution of surface moisture content under wet conditions, and since the wetter areas tended to persist during interstorm periods, these factors may also explain the increase in variance and positive skewness as field-mean moisture content decreased.

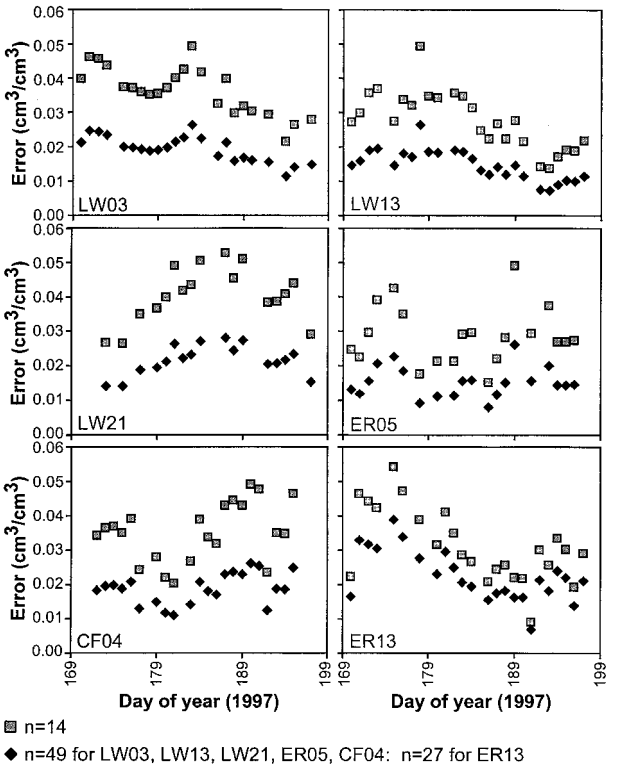

Figure 9. Error in estimated mean (cm^3/cm^3) for 14 and 27 or 49 samples versus date for each of the six fields.

5.2. Implications for Remote Sensing and Hydrological Modeling

This study has provided six locations within the SGP97 region at which the mean moisture content is known with a high degree of certainty, relative to the remaining 43 locations, at which the mean moisture content was determined gravimetrically using only 9 to 14 samples. Figure 9 shows that when the sampling density is increased (e.g., from 14 to 49 at most of the sites), the error with which the daily mean moisture content can be determined is reduced by as much as a factor of 2 (using observed standard deviations, standard limit of error equations, and $\alpha = 95\%$). Consequently, this investigation will allow for a more rigorous evaluation of ESTAR performance at these six sites. Because the different combinations of soil types, vegetation cover, and rainfall amounts at the six fields were broadly representative of those throughout the SGP97

region, understanding sensor performance at these locations should also provide insight into its capabilities across the entire study area.

A second implication of this work is that the observed relationships between variability and mean moisture content provide a means for extrapolating this information beyond the six sites. For example, spatial fields of the coefficient of variation and the standard deviation could be derived by fitting an exponential function to the coefficient of variation–mean moisture content relationship shown in Figure 5b and solving for either the coefficient of variation or the standard deviation at each 0.8-km grid cell on land given its remotely sensed mean moisture content. Such higher-order statistical information will enhance the utility of remotely sensed soil moisture to the modeling community, for example, by providing coarse estimates of soil moisture variability for models of Earth system processes operating at subgrid scales.

Finally, the dynamics of surface moisture content distributions characterized by this investigation will aid in the development of hydrological and land surface models, which often parameterize the distribution of surface moisture content statistically [e.g., *Entekhabi and Eagleson*, 1989; *Famiglietti and Wood*, 1991, 1994; *Wetzel and Boone*, 1995; *Bonan*, 1996; *Stieglitz et al*., 1997]. Until now, however, little field evidence has been available to guide developers in the choice of distribution form and to provide an understanding of its evolution through time. While modelers often choose one distribution (e.g., normal) and assume that it represents spatial variability in moisture content across a full range of wetness conditions, our work indicates that both the form of the distribution and its parameters change systematically with average moisture content. On the basis of field observations described in this paper, it appears that appropriate choices for modeling soil moisture distributions may include a normal distribution evolving into a three-parameter gamma distribution as the soil dries between storm events or a flexible distribution such as a beta distribution that can change form from negatively skewed to positively skewed with a corresponding change in its parameters.

6. Summary

The purpose of this investigation was to characterize variability in surface moisture content within six 0.8-km remote sensing footprint-sized fields during SGP97. Volumetric moisture content in the 0- to 6-cm surface soil layer was measured nearly every day at 49 points on a 7 by 7 100-m grid at five of the six fields and at 27 points on a 3 by 8 100-m grid on the sixth field. On selected days, additional higher-resolution grid or transect measurements were made on most fields. The wide spatial distribution of the sites, combined with the intensive, near-daily monitoring, provided a unique opportunity, relative to previous smaller-scale and shorter-duration soil moisture studies, to characterize variations in surface moisture content over a range of wetness conditions. Results indicated that distinct differences in mean moisture content between the six sites were consistent with variations in soil type, vegetation cover, and rainfall gradients. Within fields the standard deviation, coefficient of variation, skewness, and kurtosis increased with decreasing moisture content; the distribution of surface moisture content evolved from negatively skewed/nonnormal under very wet conditions, to normal in the midrange of mean moisture content, to positively skewed/nonnormal under dry conditions; agricultural practices of row tilling and terracing were shown to exert a major control on observed moisture content variations. Results presented here can be utilized to better evaluate ESTAR performance, to estimate subgrid-scale variations in moisture content across the entire SGP97 region, and in the parameterization of soil moisture dynamics in hydrological and land surface models.

Acknowledgments. The authors thank the many SGP97 participants, too numerous to list, that assisted with the data collection. This study would not have been possible without their efforts. We also thank the staff of the USDA ARS facilities at the Little Washita watershed and the Grazinglands Research Lab and of the DOE ARM/CART central facility. The support of NASA grants NAGW-4097 and 5240, NSF grant GER-9454098, and the University of Texas Geology Foundation is gratefully acknowledged.

References

Bell, K. R., B. J. Blanchard, T. J. Schmugge, and M. W. Witczak, Analysis of surface moisture variations within large field sites, *Water Resour. Res*., *16*, 796–810, 1980.

Bonan, G. B., A land surface model (LSM version 1.0) for ecological, hydrological, and atmospheric studies: Technical description and user's guide, *NCAR Tech. Note NCAR/TN-417+STR*, Natl. Cent. for Atmos. Res., Boulder, Colo., 1996.

Charpentier, M. A., and P. M. Groffman, Soil moisture variability within remote sensing pixels, *J. Geophys. Res*., *97*, 18,987–18,995, 1992.

Entekhabi, D., and P. Eagleson, Land surface hydrology parameterization for atmospheric general circulation models models including subgrid scale spatial variability, *J. Clim*., *2*, 816–831, 1989.

Famiglietti, J. S., Ground-based soil moisture data collection during SGP97 and current research activities, paper presented at 14th Conference on Hydrology, 79th Annual Meeting, Am. Meteorol. Soc., Dallas, Tex., Jan. 10–15, 1999.

Famiglietti, J. S., and E. F. Wood, Evapotranspiration and runoff from large land areas: Land surface hydrology for atmospheric general circulation models, *Surv. Geophys*., *12*, 179–204, 1991.

Famiglietti, J. S., and E. F. Wood, Multiscale modeling of spatially variable water and energy balance processes, *Water Resour. Res*., *30*, 3061–3078, 1994.

Famiglietti, J. S., J. W. Rudnicki, and M. Rodell, Variability in surface moisture content along a hillslope transect: Rattlesnake Hill, Texas, *J. Hydrol*., *210*, 259–281, 1998.

Francis, C. F., J. B. Thornes, A. Romero Diaz, F. Lopez Bermudez, and G. C. Fisher, Topographic control of soil moisture, vegetation cover and land degradation in a moisture stressed Mediterranean environment, *Catena*, *13*, 211–225, 1986.

Gaskin, G. J., and J. D. Miller, Measurement of soil water content using a simplified impedance measuring technique, *J. Agric. Eng. Res*., *63*, 153–160, 1996.

Hawley, M. E., T. J. Jackson, and R. H. McCuen, Surface soil moisture variation on small agricultural watersheds, *J. Hydrol*., *62*, 179–200, 1983.

Henninger, D. L., G. W. Peterson, and E. T. Engman, Surface soil moisture within a watershed: Variations, factors influencing, and relationships to surface runoff, *Soil Sci. Soc. Am. J*., *40*, 773–776, 1976.

Hills, T. C., and S. G. Reynolds, Illustrations of soil moisture variability in selected areas and plots of different sizes, *J. Hydrol*., *8*, 27–47, 1969.

Jackson, T. J., and D. E. LeVine, Mapping surface soil moisture using an aircraft-based passive microwave instrument: Algorithm and example, *J. Hydrol*., *184*, 85–99, 1996.

Jackson, T. J., and T. J. Schmugge, Passive microwave remote sensing for soil moisture: Some supporting research, *IEEE Trans. Geosci. Remote Sens*., *27*, 225–235, 1989.

LeVine, D. M., A. J. Griffiths, C. T. Swift, and T. J. Jackson, ESTAR: A synthetic aperture microwave radiometer for remote sensing applications, *Proc. IEEE*, *82*, 1787–1801, 1994.

Loague, K., Soil water content at R-5, 1, Spatial and temporal variability, *J. Hydrol*., *139*, 233–251, 1992.

Miller, J. D., G. J. Gaskin, and H. A. Anderson, From drought to

flood: Catchment responses revealed using novel soil water probes, *Hydrol. Processes*, *11*, 533–541, 1997.

Nyberg, L., Spatial variability of water content in the covered catchment at Gardsjon, Sweden, *Hydrol. Processes*, *10*, 89–103, 1996.

Owe, M., E. B. Jones, and T. J. Schmugge, Soil moisture variation patterns observed in Hand County, South Dakota, *Water Resour. Bull*., *18*, 949–954, 1982.

Rao, R. G. S., and F. T. Ulaby, Optimal spatial sampling techniques for ground truth data in microwave remote sensing of soil moisture, *Rem. Sens. Environ*., *6*, 289–301, 1977.

Reynolds, S. G., A note on the relationship between size of area and soil moisture variability, *J. Hydrol*., *22*, 71–76, 1974.

Robinson, M., and T. J. Dean, Measurement of near surface soil water content using a capacitance probe, *Hydrol. Processes*, *7*, 77–86, 1993.

Stieglitz, M., D. Rind, J. Famiglietti, and C. Rosenzwieg, An efficient approach to modeling the topographic control of surface hydrology for regional and global climate modeling, *J. Clim*., *10*, 118–137, 1997.

Wei, M., Soil Moisture: Report of a Workshop Held in Tiburon, California, 25–27 January 1994, *NASA Conf. Publ*., *3319*, 77 pp., 1995.

Wetzel, P. J., and A. Boone, A parameterization for land-atmosphere-cloud exchange (PLACE): Documentation and testing of a detailed process model of the partly cloudy boundary layer over heterogeneous land, *J. Clim*., *8*, 1810–1837, 1995.

J. A. Devereaux, J. S. Famiglietti, S. T. Graham, and M. Rodell, Department of Geological Sciences, University of Texas at Austin, Austin, TX 78712. (jdev@mail.utexas.edu; jfamiglt@maestro.geo.utexas.edu; steveg@mail.utexas.edu; mattro@mail.utexas.edu)

P. R. Houser, Hydrological Sciences Brance and Data Assimilation Office, NASA Goddard Space Flight Center, Greenbelt, MD 20771. (houser@dao.gsfc.nasa.gov)

T. J. Jackson, Hydrology Laboratory, Agricultural Research Service, U.S. Department of Agriculture, Beltsville, MD 20705. (tjackson@hydrolab.arsuda.gov)

C. A. Laymon, Institute for Global Change Research and Education, Global Hydrology and Climate Center, Huntsville, AL 35806. (Charles.Laymon@msfc.nasa.gov)

T. Tsegaye, Department of Plant and Soil Science, Alabama A & M University, Normal, AL 35762. (ttsegaye@asnaam.aamu.edu)

P. J. van Oevelen, Department of Water Resources, Wageningen Agricultural University, 6700 EK Wageningen, Netherlands. (nduiss@worldaccess.nl)

(Received August 10, 1998; revised February 8, 1999; accepted February 11, 1999.)